Ann. Occup. Hyg., Vol. 57, No. 2, pp. 261–277, 2013

doi:10.1093/annhyg/mes060

Dustiness of Fine and Nanoscale Powders

DOUGLAS E. EVANS*, LEONID A. TURKEVICH, CYNTHIA T. ROETTGERS, GREGORY J. DEYE AND PAUL A. BARON†.

National Institute for Occupational Safety and Health, Chemical Exposure and Monitoring Branch, Division of Applied Research and Technology, 4676 Columbia Parkway, MS-R7, Cincinnati, OH 45226, USA

Received 29 December 2011; in final form 20 July 2012; published online 12 October 2012

Dustiness may be defined as the propensity of a powder to form airborne dust by a prescribed mechanical stimulus; dustiness testing is typically intended to replicate mechanisms of dust generation encountered in workplaces. A novel dustiness testing device, developed for pharmaceutical application, was evaluated in the dustiness investigation of 27 fine and nanoscale powders. The device efficiently dispersed small (mg) quantities of a wide variety of fine and nanoscale powders, into a small sampling chamber. Measurements consisted of gravimetrically determined total and respirable dustiness. The following materials were studied: single and multiwalled carbon nanotubes, carbon nanofibers, and carbon blacks; fumed oxides of titanium, aluminum, silicon, and cerium; metallic nanoparticles (nickel, cobalt, manganese, and silver) silicon carbide, Arizona road dust; nanoclays; and lithium titanate. Both the total and respirable dustiness spanned two orders of magnitude (0.3–37.9% and 0.1–31.8% of the predispersed test powders, respectively). For many powders, a significant respirable dustiness was observed. For most powders studied, the respirable dustiness accounted for approximately one-third of the total dustiness. It is believed that this relationship holds for many fine and nanoscale test powders (i.e. those primarily selected for this study), but may not hold for coarse powders. Neither total nor respirable dustiness was found to be correlated with BET surface area, therefore dustiness is not determined by primary particle size. For a subset of test powders, aerodynamic particle size distributions by number were measured (with an electrical low-pressure impactor and an aerodynamic particle sizer). Particle size modes ranged from approximately 300 nm to several micrometers, but no modes below 100 nm, were observed. It is therefore unlikely that these materials would exhibit a substantial sub-100 nm particle contribution in a workplace.

Keywords: aerosolization; dustiness; dust generation; emissions; exposure; handling; nanomaterial; nanoparticle; nanoscale; powders; ultrafine; workplace

INTRODUCTION

Motivation

There is growing concern about the potential health impact of engineered nanomaterials (Schulte *et al*., 2008; Brouwer, 2010). Inhalation of airborne nanoparticles is a potentially significant exposure route. There is relatively little information on the nature and magnitude of aerosol releases during manufacture and handling of nanoparticles; however, recent work (Birch *et al*., 2011; Dahm *et al*., 2012) suggests that localized exposures to nanoparticles can and do occur in the workplace. Industrial production presents the potential for worker exposure, especially for those involved in the manual handling, transfer, or conveyance of these materials (Peters *et al*., 2009; Evans *et al*., 2010). Inhalation of aerosolized material is expected to be the primary

*Author to whom correspondence should be addressed.
†Deceased.
Tel: ++ 1 (513) 841 4407; fax: ++ 1 (513) 841 4545;
e-mail: dje3@cdc.gov

route of exposure and hence of most concern although dermal, ocular, and ingestion routes may also contribute. Controlled laboratory measurements may provide interim guidance as to the relative severity of airborne release of nanoparticles in occupational settings. Such measurements, together with information on the potential hazard (toxicity) of the material, form the basis of exposure control banding (Paik *et al*., 2008).The testing of nanoparticle powders is especially challenging, due to the small quantities of test materials available for testing (cost considerations) and the potential toxicity of these materials. This challenge is similar to that posed by potent (and frequently costly) pharmaceutical powders.

Dust generation in workplaces

A variety of airborne dust generating mechanisms may be present in the workplace. These may include accidental spills (Sutter *et al*., 1982); falling powders, via pouring or transferring processes (Heitbrink *et al*., 1992); and other agitation, as in powder conveyance (Cheng, 1973). Grinding or milling of bulk materials both generates and suspends small particles as airborne dusts (Pensis *et al*., 2010). Mechanical airborne reentrainment of previously spilled or deposited powder (perhaps through dry cleanup procedures) is also a potential source. An undesirable end result is that a portion of the bulk powder becomes and remains airborne in the workplace environment.

Dustiness testing

Dustiness has been defined as 'the propensity of a material to generate airborne dust during its handling' (Plinke *et al*., 1992; Lidén, 2006). Dustiness can be tested by 'standardized techniques' that involve the application of a specified type and amount of mechanical energy to a specified amount of test material for a specified time (in order to overcome the adhesive binding forces within the test powder) and thus disperse preexisting particles from the test powder into the air; the amount of dust released is then quantified (Plinke *et al*., 1992; Lidén, 2006). A dustiness test is not intended to generate new particles.

Lidén has argued (Lidén, 2006) that dustiness is not an intrinsic physico-chemical property of a material: the particle size distribution, humidity, and nature of the adhesive forces (binding the particles within the powder) all influence the dustiness. While the particle size distribution is not an intrinsic physico-chemical property of the material, it is a statistical property of a given powder. Humidity, for example, is an external factor that can be controlled during testing. The nature of the adhesive forces is influenced by physical form and chemistry; with appropriate control of environmental conditions (e.g. humidity), it should be possible to obtain reproducible results. Thus, while not a material property, dustiness is a property of a given powder that should be quantifiable (and reproducible) under a given controlled testing protocol.

Powders typically consist of primary particles, which are aggregated (sintered or tightly bonded) and then further agglomerated (bound by forces of varying strengths). Typically, it is fairly easy to break up the loose agglomerates (held together by van der Waals forces, for example), while breaking up the aggregates into the individual primary particles often requires considerable mechanical action (via operations like ball milling); the fracture or further diminution of primary particle size can only be achieved with extreme difficulty.

The intent behind dustiness testing is that the energy supplied should not be enough to divide the primary particles (e.g. by grinding, cutting, or crushing) within aggregates, but liberate some fraction of the loosely bound preexisting primary particles and agglomerates from the bulk powder. The fraction of airborne dust liberated from the bulk powder will be related to the chosen test conditions. The more energetic the testing protocol, the greater the fraction of airborne dust liberated from the test powder. The object of the test should be to mimic the energy supplied in a typical environmental or occupational setting, so that an assessment can be made of exposure. However, the test should be controllable and should not be subject to undue influence of uncontrolled external parameters.

Dustiness testing should be able to provide a comparison of the relative dust exposure potential of different materials. In practice, it should alert the potential for worker exposure, predict the level of that exposure, and therefore indicate a required level of control to reduce or eliminate that exposure (Heitbrink *et al*., 1989; Heitbrink *et al*., 1990; Mark, 2005; Brouwer *et al*., 2006; Pensis *et al*., 2010). Heitbrink *et al*. (1989) correlated dustiness measurements and worker exposure through bag packing; the results from dustiness tests were used to predict order of magnitude of worker exposures. A simulated workplace study of scooping/weighing/adding and cleaning/sweeping of powders by Brouwer *et al*. (2006) found that dustiness was a major determinant of worker exposure and accounted for approximately 70% of exposure

variability. Dustiness has also been suggested to be relevant for assessing the potential risk of dust explosions (Cashdollar, 2000; Turkevich *et al*., in preparation).

Historical dustiness tests

A variety of methods have historically been utilized to measure dustiness. The BOHS Working Group has described many of these methods (BOHS, 1985). Several attempts have been made at standardization (ASTM, 1980; DIN, 1999 and 2006), but these have not been widely accepted. For a review of methods, see Hamelmann and Schmidt (2003, 2004, 2005).

Many of these techniques require the use of relatively large quantities of powder, typically, 10^2–10^3 grams per test (CEN, 2006). These quantities generally preclude the testing of nanoscale powders due to their prohibitive costs.

Further complicating matters is that no clear relationship has yet been established linking inhalation exposure to dustiness as determined by any of these methods (Cowherd *et al*., 1989; Heitbrink *et al*., 1989, 1990; Class *et al*., 2001; Breum *et al*., 2003; Brouwer *et al*., 2006; Petavratzi *et al*., 2006; Tsai *et al*., 2011). While dustiness is one factor related to worker exposure potential, the quantity of material, type of operation (energy), differences in worker practice, use of exposure controls, and environmental conditions (e.g. humidity, ventilation) may also play a significant role for example, and it may be difficult to account or control for all of these factors.

Historically, dustiness testing has utilized configurations that have imparted fairly gentle mechanical agitation to the powder. These tests have been devised to simulate various industrial procedures. These configurations also tend to require larger quantities of material (>10 g), and the aerodynamics tend to involve large-scale eddies.

These methods can be qualitatively divided into two classes:

1. *Falling powder*, where a bolus of particles is released from a height (DIN, 1999). The particles are aerosolized either by the countercurrents generated during the fall or by the countercurrents generated by the impact of the bolus at the bottom of the fall (Andreasen *et al*., 1939; Hammond, 1980; BOHS, 1988; Cowherd *et al*., 1989; Plinke *et al*., 1991; Heitbrink *et al*., 1992; Cawley and Leith, 1993; Plinke *et al*., 1995).
2. *Rotating drum*, where a powder is rotated within a drum with internal baffles, so that the substrate angle periodically increases; the powder exceeds its angle of repose, and a local avalanche ensues, which aerosolizes the particles (Chung and Burdett, 1994; Hjemsted and Schneider, 1996a,b; Breum *et al*., 1997; Breum, 1999). This forms the basis of the Heubach method (DIN, 2006). Relevant to the study of nanomaterials, Schneider and Jensen (2008) scaled down the EN 15051 rotating drum apparatus (CEN, 2006) so that only several grams of powder were required per test.

These methods have been compared by various groups using a variety of powders (Heitbrink 1990; Carlson *et al*., 1992; Plinke *et al*., 1992; Bach and Schmidt, 2008; Schneider and Jensen, 2008; Jensen *et al*., 2009). Modeling of the aerosolization and dust generation of powders has also been attempted (Plinke *et al*., 1994a,b; Lanning *et al*., 1995; Ibaseta *et al*., 2008).

European standard EN 15051 (CEN, 2006) specifies two reference test methods for dustiness testing (the rotating drum and continuous falling powder tests). The rotating drum method is frequently employed due to its ability to simulate a wide range of workplace material handling processes (Mark 2005; Petavratzi *et al*., 2006). In both methods, the energy provided for aerosolization is gravity driven and possibly enhanced by agglomerate impact. The maximum velocities of the particles achieved are $v \sim 1$ m s^{-1}.

Venturi aerosolization

A qualitatively different method was introduced (Boundy *et al*., 2006) in order to test pharmaceutical powders. The aim was to utilize small quantities (~5 mg) of powder under confined conditions (cost considerations and reproducibility, and also so as not to expose the test operator to potentially toxic or pharmacologically active material). A powder is placed in a holding tube ($d = 0.44$ cm) exterior to but piercing the dispersion chamber. Air is introduced into the dispersion chamber (5.7 l) via the holding tube at a volumetric flow rate $Q = 60$ l min^{-1}, resulting in nozzle air flow v ~70 m s^{-1}. Aerosolization presumably occurs via aerodynamic lift and pneumatic drag mechanisms acting on the powder; particulate velocities are one to two orders of magnitude larger than the gentler falling powder and rotating drum methods discussed above. In addition, the aerosolization proceeds under turbulent conditions (Reynolds number, $Re = Qd/vA$ ~8000, where Q is the volumetric flow rate, d and A the tube diameter and cross-sectional area, respectively, and v

the kinematic viscosity), whereas in the gentle tests, the airflows can be considered at larger scale and in the laminar regime. For a small number of the more cohesive powders, impaction residue has been detected on the far wall of the chamber (see Fig. 2h for example), but it is not believed that this mechanism significantly contributes to the aerosolized dust.

The method provides reproducible results and is relatively quick and easy to use (Boundy *et al.*, 2006). The method does involve more aggressive air flows than those typically encountered in large-scale workplace activities, but is expected to resemble energetic dust dispersion activities (e.g. the use of compressed air to clean contaminated worker clothing or work surfaces).

There were two objectives to this study. The first was to better characterize the Venturi device, through video photography and direct reading respirable mass measurements (described in the methods section). The second objective was to rank a variety of fine and nanoscale powders according to their airborne dust generating abilities. The relationship between dustiness, and the properties of humidity, BET specific surface area and particle size was additionally investigated.

METHODS

Venturi dustiness testing device

The Venturi dustiness device, utilized in these dustiness measurements, has been described in detail elsewhere (Boundy *et al.*, 2006) but is briefly discussed below. A photograph of the chamber (without the humidity preconditioning antechamber) is presented in Fig. 1.

Air is introduced into the chamber via a side port penetrated by a metallic 'tee' shaped Venturi nozzle (Fig. 1 right); powder is placed in the vertical tube of the 'tee' (removable cap at top) and falls down the tube to reside somewhere on the curved base of the vertical tube. When air is introduced into the chamber, the primary flow is along the horizontal tube of the 'tee', although a small flow is also drawn down the vertical tube of the 'tee' (the cap is perforated by a small pinhole). This combined air flow (60 l min^{-1} at injection) aerosolizes the powder and sweeps it into the chamber.

Air is removed from the chamber (V = 5.7 l) via three ports in the top: out flows (4.2 l min^{-1}) through the cyclone (top left port) and (2.0 l min^{-1}) through the cassette (top right port) are continuous throughout the test; a third outflow (53.8 l min^{-1}) through the

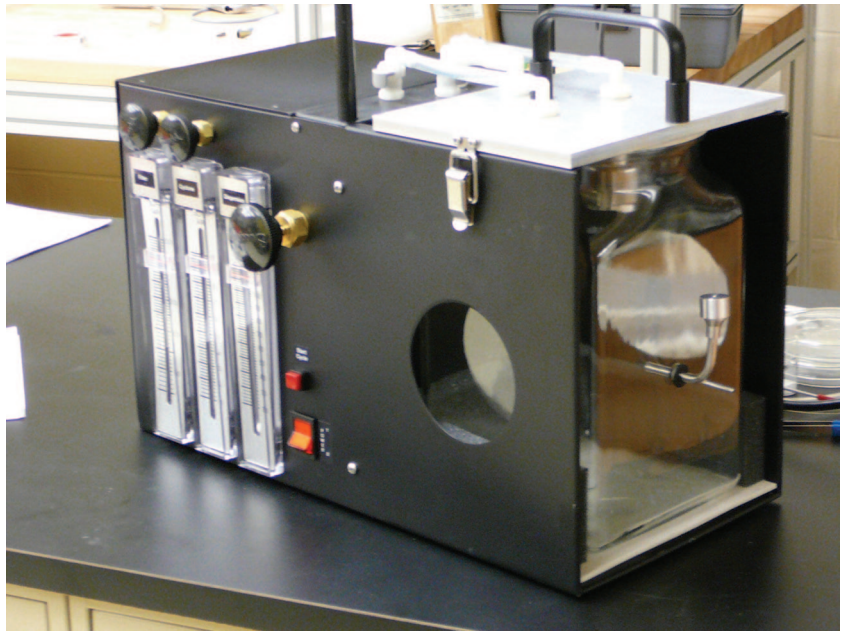

Fig. 1. The Venturi dustiness testing device used in this study.

central top port (observed to the left of the handle) occurs only during injection. Injection thus occurs at 60 l min^{-1} for 1.5 s; dust is collected for 4 min following injection, with the flow divided between the cassette and cyclone filters.

Humidity control and the antechamber

Experiments were conducted in Cincinnati OH, USA, which presented large seasonal variations in ambient laboratory humidity (dry winter, humid summer). It is well recognized that humidity or moisture content of powders can affect their dustiness (Plinke *et al*., 1995), so controlling for such effects is prudent. This was achieved in two steps. Firstly, small batches of each powder were added to clean glass vials and allowed to sit within a temperature controlled oven set to 50°C overnight, prior to weighing, to remove residual moisture. Secondly, a humidity-controlled antechamber, adjacent to the dustiness testing device, with glove and access ports and constructed from static dissipative acrylic (Plexiglas), was utilized to condition powder samples prior to dispersion (for at least 1 h) at the desired humidity.

An alternative approach that is stipulated in EN 15051 (CEN, 2006) would be to test powders in the moisture state in which they arrive. The 'as received' approach is important for determining dustiness of powders from a particular stage of a process; under that protocol, sealed samples are sent directly to the laboratory for testing without further conditioning. Moisture content for each material is then determined and reported (CEN, 2006). While different humidity conditions may be relevant for different workplaces or operations, it is important that changes in humidity, which might alter the cohesive forces in the powder, be controlled for testing, so as not to introduce additional variation in the dustiness values. In our study, the goal was to investigate dustiness without moisture introducing additional variability.

In our experiments, humidities of 20, 50, and 80% (±5%) were achieved, by selective mixing of dry and (water) saturated air, fed into the antechamber by needle valves, followed by high efficiency particulate air filtration. The antechamber additionally served as a clean conditioned environment from which air was drawn into the dustiness chamber (through the metallic 'tee') during dispersion and sampling. The clean conditioned air is of lesser importance for mass measurements, but for number concentration measurements, this step is crucial to ensure a sufficiently low particle background. Flow into the antechamber was controlled so that a slight positive pressure was attained, ensuring negligible ambient air infiltration.

Flow control

The dustiness tester was connected either to house vacuum or to two vacuum pumps connected through a vacuum regulator and gauge. Dispersion and sampling flows were controlled through needle valves built into the tester. Flow timing was automatically controlled within the tester by timed relays and solenoid valves. Sampling flows were calibrated each day using a Gilibrator and adjusted to 2.0 l min^{-1} for the closed-face metallic Slaton filter cassette, for total aerosol, and 4.2 l min^{-1} for the metallic BGI GK 2.69 cyclone with filter cassette, conforming closely to the ISO respirable sampling convention (Kenny and Gussman, 1997).

Powder and Filter Weighing

An individual test consisted of two consecutive 5 mg dispersions (totaling 10 mg of powder dispersed for each test) sampled onto the same filter media. The two 5 mg aliquots of powder were added to two aluminum weighing boats, using a microbalance (Mettler AT20, Columbus, OH), and stored and transported via glass Petridishes prior to nozzle loading. The balance was situated within a constant humidity-controlled weighing enclosure. Filters (37 mm polyvinylchloride) were pre- and postweighed using the same microbalance and transported in clean static dissipative filter holders. Each test batch typically consisted of three consecutive individual tests, with two aliquots of powder (and two filters) required per test; two additional blank filters served as a control, totaling six aliquots of powder and eight filters per batch. Preweighed powders were conditioned within the antechamber to the tester for at least 1 h prior to loading the nozzle for the first test. Six tests were typically performed for most powdered materials.

Cleaning

The chamber, nozzle, and samplers were cleaned between each test with an ultra-low penetration air filtered vacuum and wiping. A more thorough cleaning procedure, involving water, mild detergent, and isopropyl alcohol was used whenever a new test powder was introduced. A thorough description of the standard operating procedure is provided in Boundy *et al*. (2006).

Data processing

Initial dispersed masses, M_{disp}, were measured with weigh boats prior to loading in the holding tube; masses, M_{cycl} and M_{cass}, determined from pre- and

postweighed filter media, were blank corrected. Total dustiness, D_{tot}, and respirable dustiness, D_{resp}, were determined as follows:

$$D_{tot} = \left(\frac{M_{cass}}{M_{disp}}\right) \times \frac{f_{cycl} + f_{cass}}{f_{cass}} \quad (1)$$

$$D_{resp} = \left(\frac{M_{cycl}}{M_{disp}}\right) \times \frac{f_{cycl} + f_{cass}}{f_{cycl}} \quad (2)$$

where f_{cycl} and f_{cass} are the flow rates through the cyclone and cassette, respectively. The above ratios (mass of aerosolized dust to mass of loaded powder) are converted to percentages with multiplication by a factor of 100. Dustiness results are typically expressed as mg kg^{-1} elsewhere (i.e. normalized in some way to the amount of starting material).
Statistical analyses of the dustiness results were performed within Microsoft Excel.

Video photographic documentation of the dispersion

The dispersion of several powders was video-photographed (SONY HandyCam DCR-VX 2000 with 3CCD progressive scan) at 30 frames s^{-1} to visualize the aerosolization and mixing processes within the transparent glass chamber. Figure 2 presents the progression of one such dispersion of Aeroxide P25 fumed TiO_2: the injection 'tee' is to the right of each figure, the back wall of the glass chamber is to the left, the cyclone protrudes at top upper left and the closed-face cassette can be observed upper right. Figure 2a (t = 0.03 s) documents the initiation of injection: a light is illuminated from the right whose reflection (white with blue halo) is visible on the back wall of the chamber at left; at this moment, all three flows (2.0 l min^{-1}, 4.2 l min^{-1}, 53.8 l min^{-1}) are open. Figure 2b (t = 0.07 s) documents the powder jet emerging from the injection 'tee'. Figure 2c (t = 0.10 s) shows the spreading of the powder jet. Figure 2d (t = 0.13 s) shows continued spreading of the powder jet; streamers of heavier particles (large agglomerates) can be seen at the bottom of the cloud. Figs 2e,2f,2g (t = 0.17, 0.20, 0.23 s) show continued spreading of the powder jet. In Fig. 2h (t = 0.27 s), impacted powder residue can be seen on the back wall (just below the illuminating light); such impacted material has been observed for only a small number of powders, and it is believed that this mechanism does not contribute significant material to the dust cloud. In Fig. 2i (t = 0.33 s), the powder cloud has dispersed throughout the chamber, and clean air, introduced by the injection tube, clarifies the central portion of the chamber. The dust cloud in the chamber mixes, and, in Fig. 2j (t = 0.77 s), a momentary second injection (of very fine material) seems to have occurred. The dust cloud continues to mix. In the final frame, Fig. 2k (t = 1.50 s), the injection air (53.8 l min^{-1}) has ceased; however, in Fig. 2l (t = 1.53 s), a final particle jet occurs (probably material dislodged by the momentary backflow when the 53.8 l min^{-1} injection air flow is closed off, but which is then swept into the chamber by the remaining 6.2 l min^{-1}). While the injection process is complicated, even within this relatively simple geometry and protocol, it is clear that in this test, aerosolization of the test powder occurs under considerably more energetic flow conditions than with dustiness tests previously described (rotating drum and continuous falling powder).

Photometer time series

The time evolution of the dust cloud was monitored in the following experiment with carbon nanofibers (Pyrograph III). This experiment formed part of an instrument calibration assessment for a parallel workplace study (Evans *et al.*, 2010). The closed-face cassette was removed, and a photometer (DustTrak Model 8520, TSI Inc., Shoreview, MN) was connected (externally) to this port via a 3-way valve, with the 10-mm Dorr-Oliver cyclone providing a respirable size-selective inlet at 1.7 l min^{-1} within the chamber. The respirable BGI cyclone was operated simultaneously and the material collected, determined gravimetrically as per the standard protocol. Following the usual dispersion, a 3-way valve was switched, such that air was drawn from the chamber into the photometer; the total volume exchange rate during this calibration test is Q = 1.7 l min^{-1} + 4.2 l min^{-1} = 5.9 l min^{-1}. Photometer mass concentration estimates were measured and logged every second.

Figure 3 presents a time series of respirable mass concentration. The photometer measurements provided a reasonable estimate of the respirable mass concentration for these carbon nanofibers and therefore no further calibration or correction factor was required (Evans *et al.*, 2010). The exponential decay of concentration (τ = 55.6 s = 0.927 min, R^2 = 0.995) is consistent with the dominant particle loss mechanism being dilution (removal of contaminated air through sampling and replacement with clean air: $Q = V/\tau$ = 5.7 l/0.927 min = 6.2 l min^{-1}). Gravitational settling and losses to the chamber walls did not

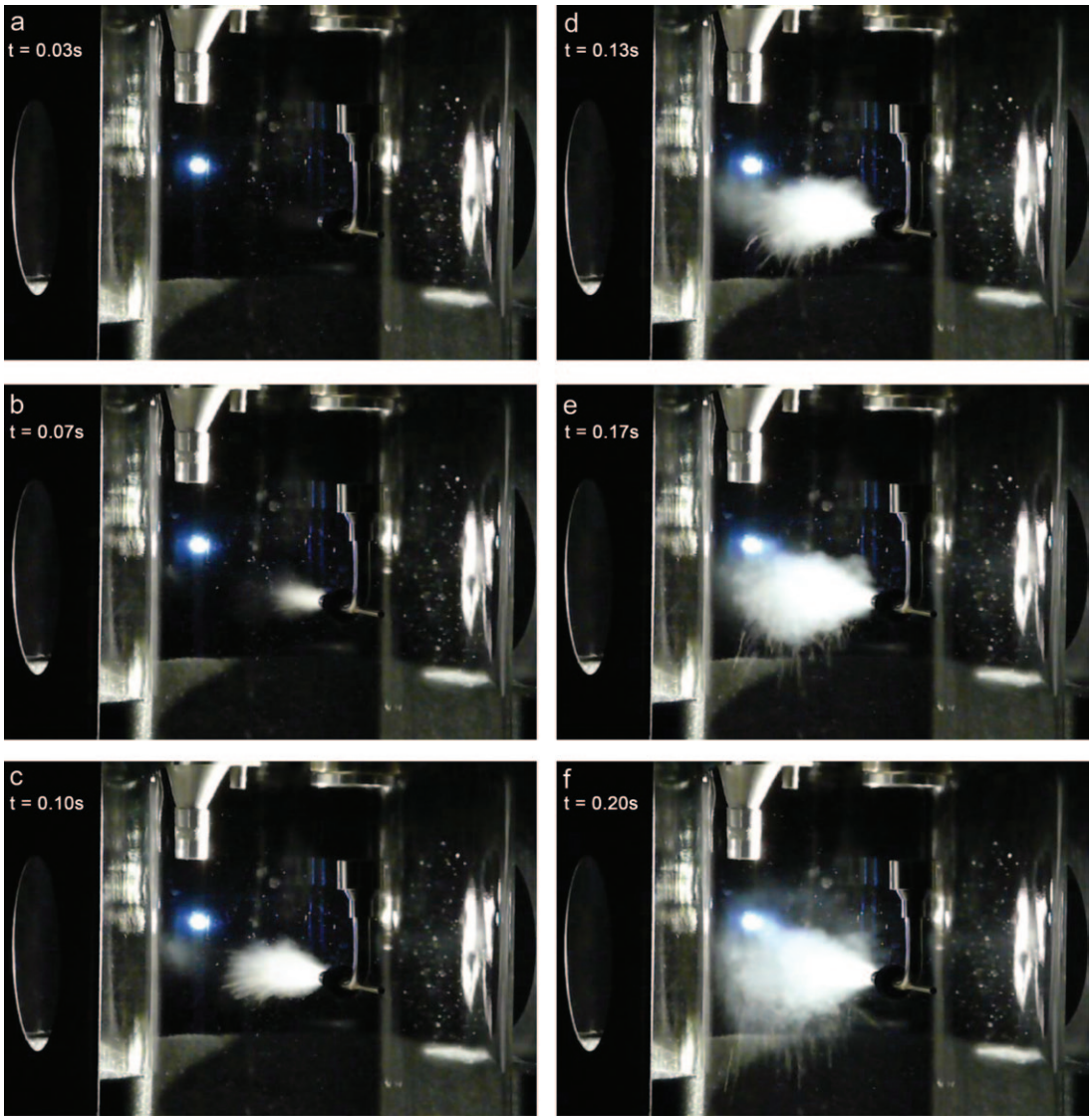

Fig. 2. Sequential photographs of the dispersion of 5 mg of Aeroxide P25 TiO_2 powder in the dustiness chamber.

appear to significantly contribute (~5%) to the concentration decay within the chamber.

Size distribution measurements

Size distribution measurements by aerodynamic diameter were conducted on a subset of the gravimetrically tested powders, using an electrical low-pressure impactor (ELPI; Dekati, Tampere, Finland) and an aerodynamic particle sizer (APS, model 3021 TSI, Shoreview, MN, USA). These measurements provided overlapping particle size distributions (by number) from 27 nm to 20 µm (ELPI, 27 nm to 10 µm and APS from 500 nm to 20 µm).

For these measurements, the two filters (cassette and cyclone) were removed and a single sampling probe was connected to both the APS and ELPI instruments; these instruments required 5 l min^{-1} and 10 l min^{-1} flows, respectively (replacing the 2 l min^{-1} through the cassette and the 4.2 1 min^{-1} through the cyclone); a static dissipative Plexiglas (instead of the standard glass) chamber was used for these measurements. In the standard configuration, the

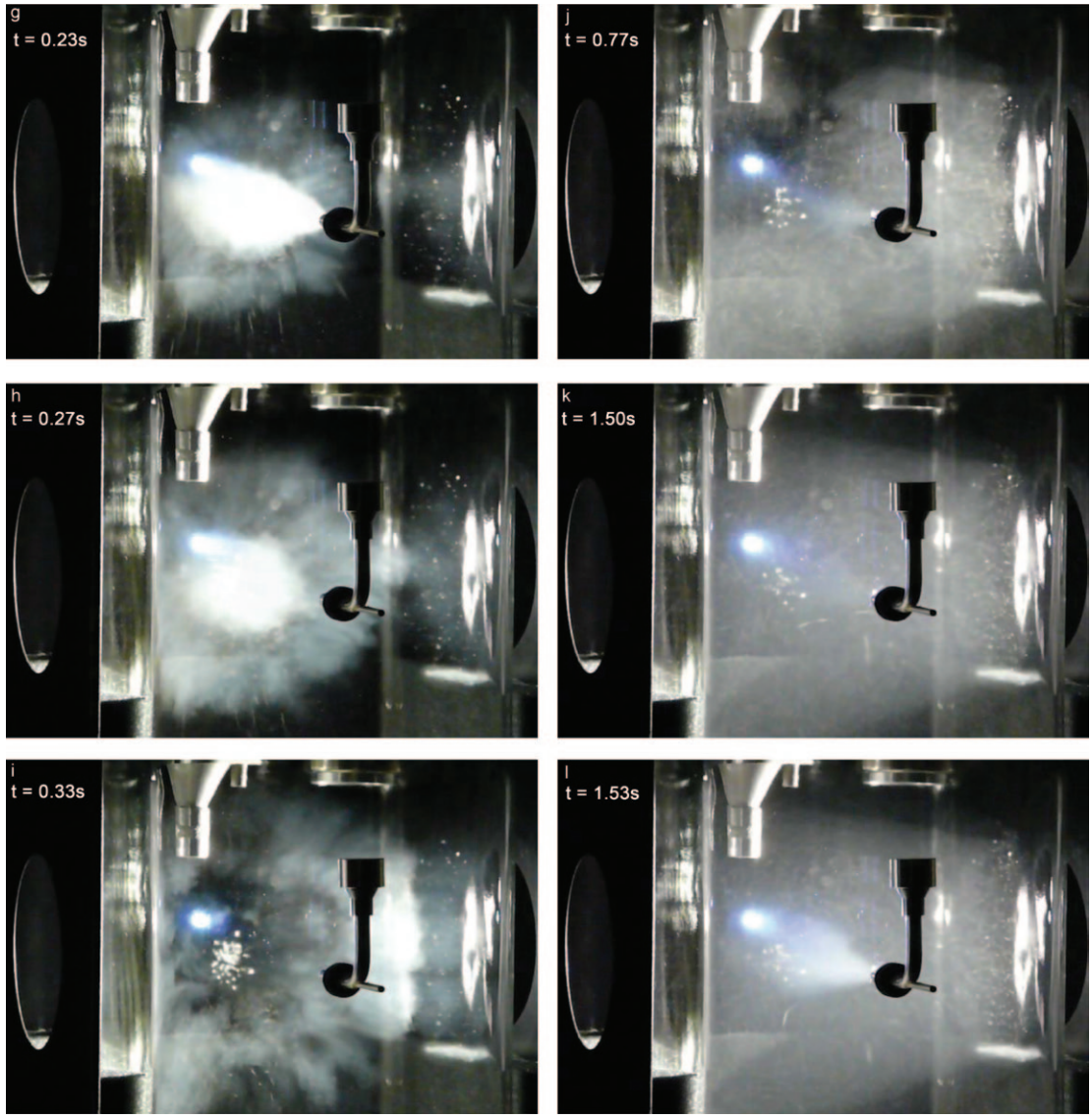

sampling (through both the cassette and the cyclone) commenced simultaneously with the powder injection; with the APS and ELPI instruments, the sampling occurred only after injection was completed. Otherwise, the test was conducted as before, but using the 3-way valve arrangement.

It should also be noted that the initial loading was reduced to 1 mg for the Pyrograf III carbon nanofibers, HiPCO single-walled carbon nanotubes (SWCNTs) and Aerosil 50 OX fumed SiO_2 samples; all other samples were loaded with 5 mg of powder for a single dispersion. Particle size distributions (number of particles as a function of aerodynamic diameter) were measured over the entire duration of the test; reported are the distributions averaged over the first minute for each instrument.

Materials

Twenty-seven powders were evaluated. Candidate materials included single- and multiwalled carbon nanotubes (MWCNTs), carbon nanofibers (CNFs), carbon blacks; oxides of titanium, aluminum, silicon, and cerium; metallic nanoparticles (nickel, cobalt, manganese, and silver), silicon carbide, Arizona road dust; nanoclays; and a mixed metal oxide, lithium titanate.

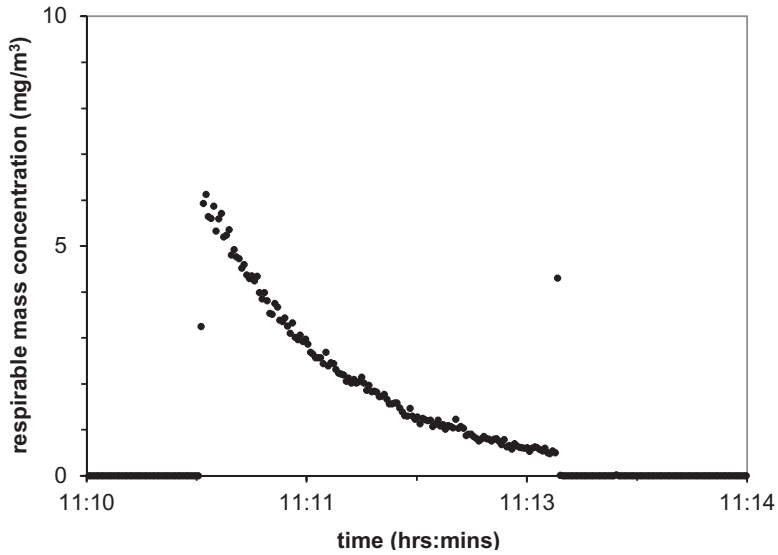

Fig. 3. Time dependence of respirable particle mass concentration (measured by a photometer) for Pyrograf III CNFs, following initial dispersion of 5 mg within the dustiness chamber.

These provided a broad array of available powders. (Details of the provenance of these materials and additional physical parameters are provided as supplementary data, available at *Annals of Occupational Hygiene* online). Specific surface areas were determined by BET analyses (Brunauer *et al*., 1938) and are listed in Table 1.

RESULTS AND DISCUSSION

Dustiness measurements

Twenty-seven fine and nanoscale materials were evaluated at 50% relative humidity (Table 1 and Fig. 4). Mean average values, and standard deviations, are provided. The lactose standard, widely utilized within the pharmaceutical industry, was included in order to make contact with the earlier work conducted with this device (Boundy *et al*., 2006). The values of D_{tot} = 5.2 (±0.4)% and D_{resp} = 0.9 (±0.1)% for the lactose in this study are fully consistent with those reported by Boundy *et al*. (2006). Since the measurements presented here were made over the course of approximately 4 years, and by several operators, the Arizona Road Dust was adopted as an internal standard to verify proper operation of the equipment.

For eight materials, total and respirable dustiness was studied as a function of relative humidity at 20, 50, and 80%. Results are presented in Table 2. With the exception of the Microgrit cerium oxide, where a marked decrease in both total and respirable dustiness was observed at the elevated relative humidity, there was no detectable variation of dustiness with humidity. While it is evident that not all powdered materials may be influenced by humidity, it is a factor that needs to be controlled during testing.

Returning to the 50% relative humidity measurements (Table 1), total and respirable dustiness varied over two orders of magnitude. This is conveniently displayed as respirable versus total dustiness using logarithmic scales (Fig. 4). Powders are color coded by material class (carbonaceous, fumed oxides, nanoscale metals, fine oxides, miscellaneous). Each material class is represented over the entire range of dustiness values (see discussion below). Error bars indicate 1 SD in the dustiness measurements. These statistical errors are typically large for low values of dustiness (lower left on Fig. 4) and small for high values of dustiness (upper right in Fig. 4). The relative mass resolution by gravimetric analysis is ~10^{-5} g, which is comparable to the statistical variability (~0.1%) in powders with low dustiness values.

The relatively small intertest variability (i.e. high consistency) for the majority of the test materials is indicative of the intrinsic reproducibility of the Venturi device. Boundy *et al*. (2006) reported similar findings. The few cases of high intertest variability are probably due to inhomogeneity of the test material (between test aliquots); test materials that

Table 1. Dustiness of fine and nanoscale test powders at 50% relative humidity. Powders are grouped in material classes and then ranked by total dustiness.

Powder	Total dustiness, D_{tot} (%)	Respirable dustiness, D_{resp} (%)	D_{resp}/D_{tot}	Specific surface area (m^2/g)
	Mean (SD)	Mean (SD)		
Carbonaceous				
SWCNT				
HiPCO	37.9 (3.4)	31.8 (3.3)	0.84	144[c] 508[a]
SWeNT	8.1	3.3	0.41	617 (3)[b]
MWCNT				
Mitsui VII	14.0 (4.3)	2.4 (0.6)	0.17	23 (0.5)[b]
CNF				
Pyrograph III	4.9 (1.0)	1.4 (0.3)	0.28	57 (0.5)[b]
Carbon Black				
Printex 90	30.9 (3.1)	12.9 (1.4)	0.42	306 (4)[b]
Std. Ref. 8	0.8 (0.2)	0.4 (0.1)	0.46	139 a 143[c]
Sterling V	0.3 (0.2)	0.2 (0.1)	0.61	37 (0.1)[b]
Fumed oxides				
SiO_2				
Aerosil 380	15.0 (3.0)	5.5 (0.5)	0.37	380[d]
Aerosil 200	7.8 (1.4)	3.3 (0.5)	0.42	200[d]
Aerosil 50 OX	3.0 (0.1)	1.5 (0.1)	0.5	50 (15)[d]
Hydrophobic SiO_2				
Aerosil R812	22.1 (0.7)	10.7 (0.4)	0.49	300[d]
Aerosil R202	16.6 (4.6)	6.2 (1.0)	0.37	100 (20)[d]
Al_2O_3				
Aeroxide Alu C	26.0 (3.2)	12.4 (2.1)	0.48	100 (15)[d]
TiO_2				
Aeroxide P25	15.7 (5.1)	7.2 (2.1)	0.46	50 (15)[d]
CeO_2				
HSL CeO_2	5.8 (0.2)	2.8 (0.3)	0.49	37 (9)[d]
Nanoscale metals				
Ni	16.7 (0.4)	7.5 (0.2)	0.45	50 (15)[d]
Co	7.2 (0.7)	2.5 (0.2)	0.35	45 (15)[d]
Mn	4.2 (0.2)	1.1 (0.1)	0.27	28 (8)[d]
Ag	1.7 (0.3)	0.4 (0.2)	0.25	20 (5)[d]
Fine oxides				
Lithium titanate spinel	11.1 (1.1)	3.4 (0.1)	0.31	135[d]
AZ road dust (SiO_2)	7.7 (1.5)	3.9 (0.8)	0.5	8.0 (0.1)[e]
Microgrit CeO_2	6.5 (2.2)	2.6 (0.8)	0.39	4.05 (0.01)[e]
Kemira TiO_2	0.3 (0.5)	0.1 (0.2)	0.4	10[d]
Miscellaneous				
Microgrit SiC	27.4 (1.0)	9.6 (0.3)	0.35	3.19 (0.02)[e]
Holland lactose	5.2 (0.4)	0.9 (0.1)	0.17	0.534 (0.006)[e]
Nanoclays				
PGN	3.9 (1.2)	0.8 (0.3)	0.21	11.29 (0.09)[e]
PGV	3.6 (0.3)	0.4 (0.1)	0.10	34.52 (0.29)[e]

Tabulated are materials tested, mean and standard deviations for both total and respirable dustiness. Dustiness is the ratio of collected to predispersed mass of powder for each test and expressed as a percentage. The D_{resp}/D_{tot} column provides the ratio of respirable to total dustiness and the final column, the specific surface area obtained by BET analysis for each material. SD, standard deviation.

[a] Shvedova *et al*. (2008).
[b] Pacific Surface Science, in Turkevich *et al.*, in preparation.
[c] Pacific Surface Science, in Ruda-Eberenz *et al*. Ann. Occup. Hyg., in press.
[d] Manufacturer's value.
[e] Pacific Surface Science, this work.

contain granular particles or clumps tend to disperse irreproducibly. Presieving (i.e. with 200 mesh) of the powders prior to testing may improve reproducibility (e.g. as described in ISO 14488, 2007). By far, the most dusty material examined was the SWCNT manufactured by the HiPCO process, with D_{tot} = 37.9 (±3.4)%, D_{resp} = 31.8 (±3.3)%. This is of particular concern, because of the high respirable fraction. Furthermore, animal studies have demonstrated significant adverse health endpoints, including inflammation, rapid pulmonary fibrosis, granulomas, oxidative stress, and mutagenesis (Shvedova *et al*., 2005, 2008; NIOSH, 2010) with this material. This motivates a higher level of exposure control for workers handling this material. Conventional exposure controls appear to be effective in reducing exposures to carbon nanotubes and nanofibers, where effectively implemented (Dahm *et al*., 2012).

The next most dusty material, the Carbon Black, Printex 90, had comparable D_{tot} = 30.9 (±3.1)%, but significantly lower D_{resp} = 12.9 (±1.4)%. It is probably noteworthy that both HiPCO SWCNTs and Printex 90 materials belong to the carbonaceous category. As we proceed to less dusty materials, all categories of materials X (D_{tot}, D_{resp}) are represented: Microgrit SiC (27.4, 9.6), AluC Al_2O_3 (26.0, 12.4), Aerosil R812 SiO_2 (22.1, 10.7), Ni (16.7, 7.5), Aerosil R202 SiO_2 (16.6, 6.2), Aeroxide P25 TiO_2 (15.7, 7.2), and Aerosil 380 SiO_2 (15.0, 5.5). No one material class stands out as being excessively dusty (i.e. significantly more dusty than the others); conversely, no one material class stands out as being relatively 'dust free'. It is instructive to examine these results by material class.

Within the carbonaceous class, total dustiness ranges from 0.3% (Sterling V) to 37.9% (HiPCO SWCNT); this represents a range of two orders of magnitude. Similarly, respirable dustiness ranges from 0.2% (Sterling V) to 31.8% (SWCNT HiPCO); again, this represents a range of two orders of magnitude. It is interesting that respirable dustiness appears to be related to total dustiness.

Within the fumed oxide class, total dustiness ranges from 3.0% (Aerosil 50 OX SiO_2) to 22.1% (Aerosil R812 SiO_2); this represents a range of one order of magnitude. Similarly, respirable dustiness ranges from 1.5% (Aerosil 50 OX SiO_2) to 10.7% (Aerosil R812 SiO_2), an order of magnitude variation.

Only four nanoscale metals were studied. The total dustiness ranges from 1.7% (Ag) to 16.7% (Ni), again, an order of magnitude range. The respirable dustiness ranges from 0.4% (Ag) to 7.5% (Ni), an order of magnitude variation.

Within the fine oxide powders, the total dustiness ranges from 0.3% (Kemira TiO_2) to 11.1% (Altair lithium titanate spinel), almost two orders of magnitude. The respirable dustiness ranges from 0.1% (Kemira TiO_2) to 3.9% (Arizona Road Dust), again more than an order of magnitude.

In the remaining miscellaneous category, the total dustiness ranges from 3.6% (nanoclay PGV)

Table 2. Humidity effect on total and respirable dustiness for select materials. Mean values and standard deviations are provided.

Relative humidity (%)	20		50		80	
Dustiness	D_{tot} (%)	D_{resp} (%)	D_{tot} (%)	D_{resp} (%)	D_{tot} (%)	D_{resp} (%)
Powder	Mean (SD)	Mean (SD)	Mean (SD)	Mean (SD)	Mean (SD)	Mean (SD).
Aeroxide P25 TiO_2	9.5 (4.9)	6.3 (1.8)	15.7 (5.1)	7.2 (2.1)	13.5 (2.3)	6.0 (1.1)
Aerosil OX 50 SiO_2	2.5 (1.4)	1.9 (0.7)	3.0 (0.1)	1.5 (0.1)	3.0 (0.6)	1.8 (0.4)
HSL CeO_2	4.9 (2.0)	2.7 (0.3)	5.8 (0.3)	2.8 (0.3)	5.8 (1.8)	1.6 (1.1)
AZ road dust (SiO_2)	7.4 (0.4)	4.2 (0.2)	7.7 (1.5)	3.9 (0.8)	7.3 (3.5)	4.0 (2.9)
Microgrit CeO_2	6.5 (0.5)	3.5 (0.5)	6.5 (2.2)	2.6 (0.8)	1.2 (0.4)	0.4 (0.1)
Microgrit SiC	—	—	27.4 (1.0)	9.6 (0.3)	25.3 (9.8)	9.6 (0.9)
PGN nanoclay	2.9 (0.1)	0.5 (0.1)	3.9 (1.2)	0.8 (0.3)	3.7 (1.9)	0.3 (0)
Printex 90 carbon	31.9 (1.8)	13.5 (0.2)	30.9 (3.1)	12.9 (1.4)	30.2 (1.5)	10.6 (1.3)
Sucrose[a]	0.1 (0.0)	0.3 (0.0)	—	—	—	—

[a]Sucrose: deliquescent for relative humidity at 50% and greater.

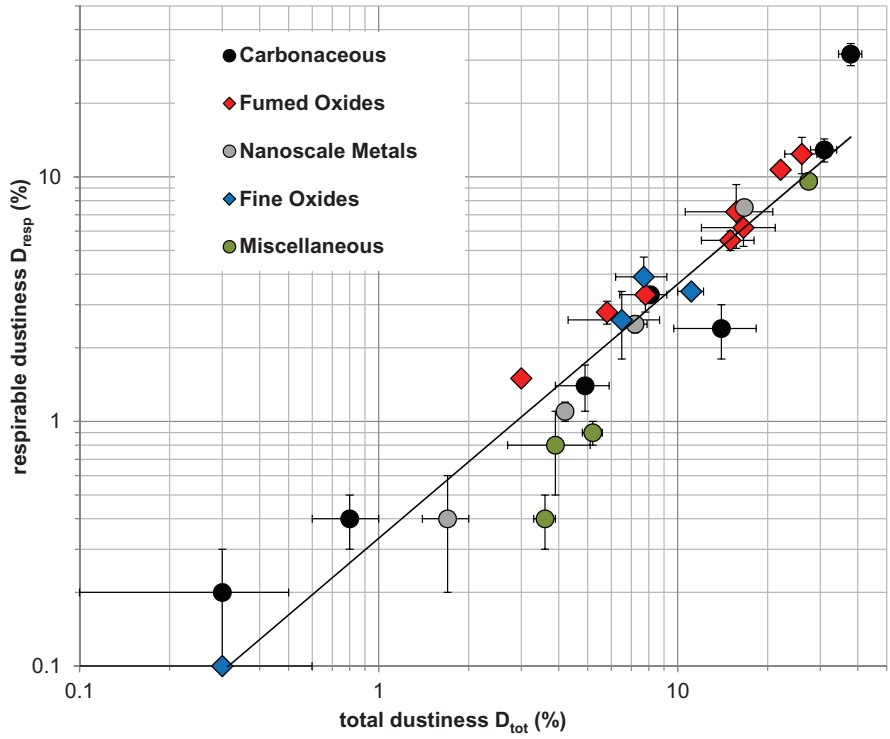

Fig. 4. Relationship between and total and respirable dustiness for 27 tested materials at 50% relative humidity. Total and respirable dustiness are each expressed as a percentage of the initial mass of predispersed test powder. Reported is the mean of multiple replicate tests with error bars representing 1 SD. Numerical data are provided in Table1.

to 27.4% (Microgrit SiC), an order of magnitude. The respirable dustiness ranges from 0.4% (nanoclay PGV) to 9.6% (Microgrit SiC), more than an order of magnitude. Again, there appears to be a relationship between total and respirable dustiness.

As anticipated, for all materials and experiments, $D_{resp} < D_{tot}$, i.e. the respirable dustiness is always less than the total dustiness (this is a nice internal check on the method, since D_{resp} and D_{tot} are obtained from independent measurements). Furthermore, total and respirable dustiness appear to be correlated. The correlation between total and respirable dustiness is made evident in Fig. 4, where respirable dustiness, D_{resp}, versus total dustiness, D_{tot}, is plotted (log-log scale). This may be fit to a power law,

$$D_{resp} \sim D_{tot}^{n} \tag{3}$$

with n = 1.04 (1 SD in the exponent, ω_n = 0.07; R^2 = 0.90). Since the exponent n ~1, the total and respirable dustiness are linearly related across the wide range of materials tested. The D_{resp}/D_{tot} column of Table 1 gives the ratio of respirable to total dustiness. For all the materials studied, D_{resp}/D_{tot} = 0.39 ± 0.15 (1 SD). Some materials studied lie outside this range. Materials with an anomalously high D_{resp}/D_{tot} ratio are HiPCO SWCNT (0.84) and Sterling V carbon black (0.61); materials with an anomalously low D_{resp}/D_{tot} ratio are Mitsui VII MWCNTs (0.17), Holland lactose (0.17), nanoclays PGN (0.21), and PGV (0.10). These anomalous materials are further discussed in the size distribution measurements below.

The linear relationship observed between respirable and total dustiness was unexpected and actually quite remarkable. This relationship is fortuitous and most likely results from the selection of materials in this study (mostly fine and nanoscale powders).

The results between the Venturi method presented here may be compared with results reported elsewhere where the same powders were tested. Tsai *et al*. (2009) reported gravimetrically determined dustiness from the rotating drum (CEN, 2006) for the Aeroxide P25

fumed TiO_2 powder: 6713 (±546), 576 (±37), and 15 (±37) mg kg^{-1} for the inhalable, thoracic, and respirable dustiness, respectively. For comparison, results from this study (Table 1) are 1.57 (±0.51) × 10^5 mg kg^{-1} for total dustiness and 7.2 (±2.1) × 10^4 mg kg^{-1} for respirable dustiness are obtained. If total dustiness (provided by the closed face cassette) crudely approximates that of the inhalable fraction, then the Venturi method yields a 20-fold larger total (inhalable) dustiness; and lastly, the Venturi respirable dustiness is three orders of magnitude greater. NIOSH has published a current intelligence bulletin on occupational exposures to TiO_2 (NIOSH, 2011).

O'Shaughnessy *et al.*, (2012) constructed a small-scale falling powder test and used APS counts to estimate respirable mass for several powders, two of which were also investigated here. They report respirable dustiness values of 45.3 (±8.5) mg kg^{-1} for Aeroxide P25 fumed TiO_2 and 42.9 (±6.0) for Printex 90 carbon black. For comparison, results from this study (Table 1) are 7.2 (±2.1) × 10^4 mg kg^{-1} for Aeroxide P25 fumed TiO_2 and 1.29 (±0.14) × 10^5 mg kg^{-1} for Printex 90 carbon black. Again, the Venturi dispersion yields respirable dustiness values three orders of magnitude larger than the small-scale falling powder values. A combination of energetic dispersion and small chamber volume (5.7 l, when compared with sampled air volume, 4 min × 6.2 l min^{-1} = 24.8 l) for the Venturi device results in efficient airborne collection. It is the energetic dispersion coupled with efficient collection within the Venturi device, which makes gravimetric dustiness determination for mg quantities of fine and nanoscale materials possible.

Relationship with BET Surface Area and Primary Particle Size. The dustiness values do not appear to be correlated with primary particle size. Primary particle size is directly related to the specific surface area provided by BET analysis (Hinds, 1999). Values for BET-derived specific surface area are provided in Table 1 for each test material. Fig. 5 displays (i) the total dustiness and (ii) the respirable dustiness, as a function of BET specific surface area. Attempts to fit to power laws resulted in the following:

$$D_{tot} \sim \mathrm{BET}^{n} \tag{4a}$$

with $n = 0.21$ ($R^2 = 0.068$), and

$$D_{resp} \sim \mathrm{BET}^{n} \tag{4b}$$

with $n = 0.32$ ($R^2 = 0.13$). There was significant scatter in this data (very poor R^2). It would thus appear that neither total dustiness, D_{tot}, nor respirable dustiness, D_{resp}, is predictable from primary particle size.

Particle Size Distribution Measurements. The D_{resp}/D_{tot} relationship (discussed earlier in the gravimetric dustiness measurements) was further studied by making aerodynamic particle size distribution measurements, by number, for a subset of powders. The size distributions (Fig. 6) are peak-normalized and are ordered by D_{resp}/D_{tot} (PGV with D_{resp}/D_{tot} = 0.10, at top, to SWCNT-HiPCO with D_{resp}/D_{tot} = 0.84, at bottom). All D_{resp}/D_{tot} values are provided in Table 1.

The APS measurements cut off below 0.5 µm. Except for the Mitsui VII MWCNTs, Pyrograf III CNFs, and HiPCO SWCNTs, the APS and ELPI results track each other very well. It is noteworthy that these three anomalous materials are all carbonaceous and display relatively complex airborne morphologies (Shvevoda *et al.*, 2008; Porter *et al.*, 2010; Ku *et al.*, 2006). It is speculated that the discrepancy between the particle size distributions, as measured by these two instruments, may arise from poor counting efficiency of the APS in the submicrometer region for optically black (absorbing) materials with complex airborne morphologies. Further experimental study is clearly warranted.

There is a general qualitative trend that materials with low (high) D_{resp}/D_{tot} have particle number distributions with modes at larger (smaller) aerodynamic diameter (Fig. 6). Unfortunately, a more quantitative relationship between D_{resp}/D_{tot} and the particle number distribution cannot be deduced. Aerodynamic particle size distribution modes range from ~300 nm to several micrometers as the D_{resp}/D_{tot} ratio increases. It is also noteworthy that no aerodynamic particle size mode below 100 nm was observed for any of the materials measured, despite the relatively energetic dispersal mechanism employed with the Venturi testing device. Thus a substantial sub-100 nm fraction is unlikely to be encountered in the workplace from these materials.

CONCLUSIONS

A novel dustiness testing device, developed for pharmaceutical application, was evaluated in this study to investigate 27 fine and nanoscale powders. The device efficiently dispersed small (mg) quantities of the test powders into a small enclosed

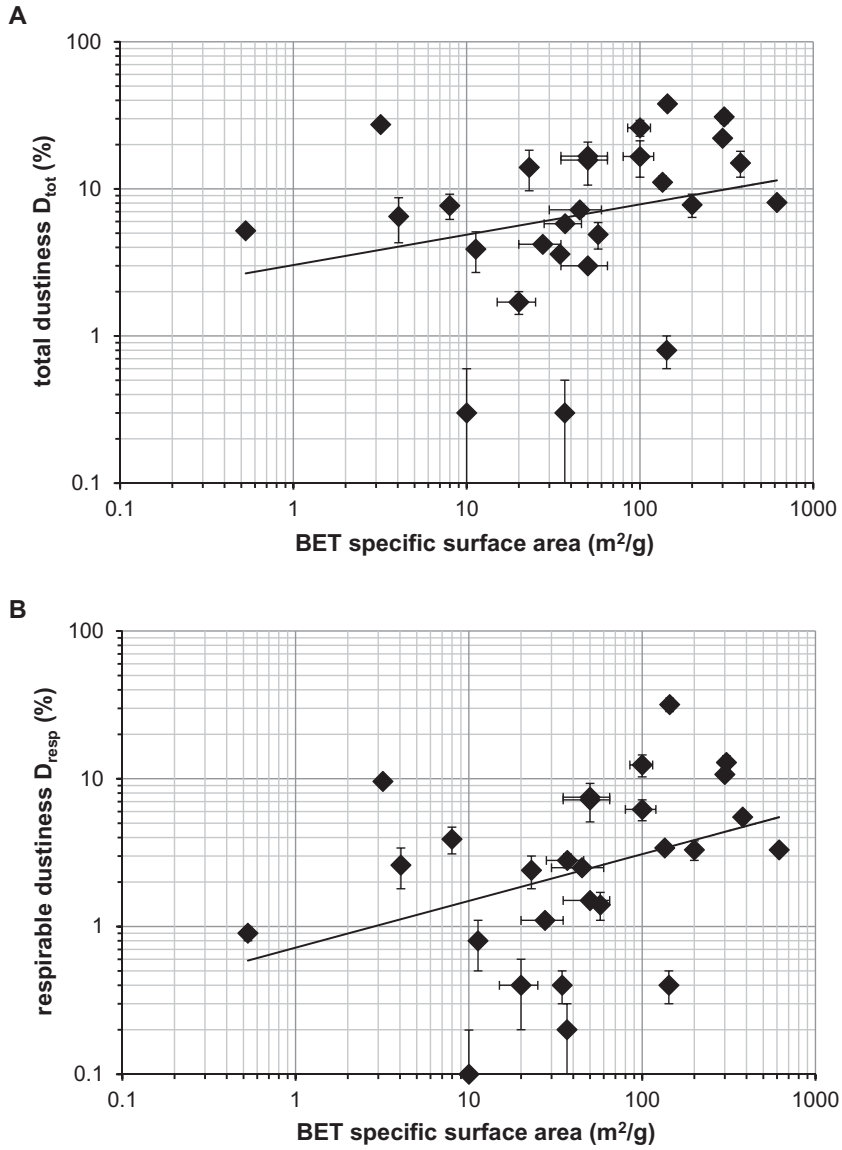

Fig. 5. (a) Relationship between total dustiness D_{tot} and BET specific surface area. (b) Relationship between respirable dustiness D_{resp} and BET specific surface area.

chamber, by utilizing an energetic Venturi aerosolization. The total and respirable dustiness were gravimetrically determined. The Venturi dispersion and subsequent particle concentration decay were studied within the dustiness chamber by video photography and a photometer time series for respirable particle mass. The aerosolization of the powder proceeds under turbulent conditions and provides a more energetic dispersion than traditional testing methods (e.g. rotating drum or continuous falling powder), but perhaps may better describe a worst case scenario in a workplace. Furthermore, the device may emulate the efficient aerosolization of powders that takes place during the (nonrecommended) practice of cleaning contaminated worker coveralls and dry work surfaces with compressed air. Respirable mass concentration (as measured by photometer) decayed

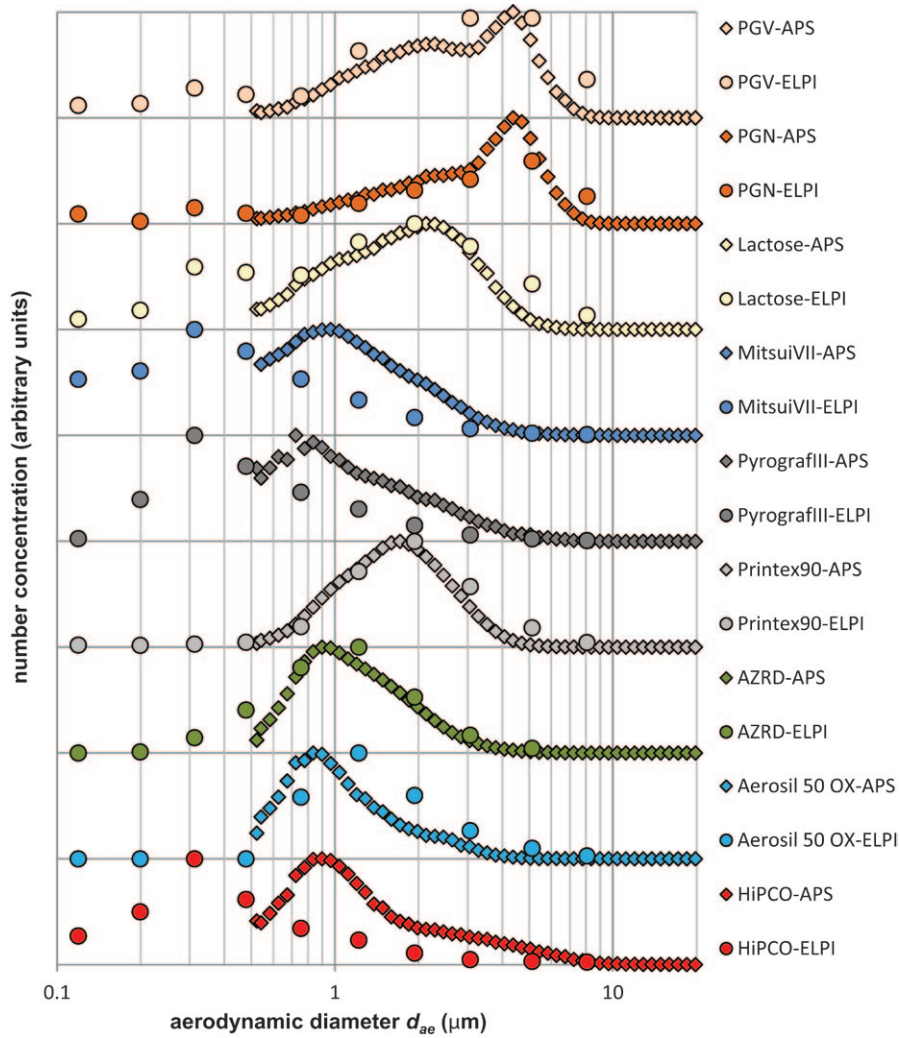

Fig. 6. Aerodynamic particle size distributions by number (provided by the ELPI and APS) for several materials with increasing D_{resp}/D_{tot}. Particle number concentrations have been peak-normalized (hence arbitrary units). The materials are ordered (top through bottom with increasing D_{resp}/D_{tot}) by nanoclays PGV and PGN, Holland Lactose, Mitsui VII MWCNT, Pyrograph III CNF, Printex 90 Carbon Black, Arizona Road Dust, Aerosil 50 OX fumed SiO_2, and HiPCO SWCNT.

exponentially, quantitatively consistent with clean air dilution within the chamber during sampling. The energetic dispersion and efficient collection within the Venturi device makes gravimetric dustiness determination of mg quantities of fine and nanoscale powders possible.

The following materials were studied: SWCNTs and MWCNTs, CNFs, carbon blacks; fumed oxides of titanium, aluminum, silicon, and cerium; metallic nanoparticles (nickel, cobalt, manganese, and silver); silicon carbide, Arizona road dust; nanoclays; and lithium titanate.

Both the total and respirable dustiness of the dispersed powders spanned two orders of magnitude (0.3–37.9% and 0.1–31.8%, respectively). For many powders, a significant respirable dustiness was observed, suggesting that workplace procedures may result in inhaled airborne dust, a significant fraction of which may be capable of reaching a worker's deep lung.

Those materials with a potentially high respirable (and total) dustiness included HiPCO SWCNTs, Printex 90 carbon black, Aerosil R812 fumed SiO_2, Microgrit SiC 1200, Alu C fumed Al_2O_3, QSI nickel, Aeroxide P25 fumed TiO_2,

Aerosil R202 and 380 fumed SiO_2. It is noteworthy that many of the potentially high respirable dustiness materials comprise the fumed oxides (SiO_2, TiO_2, and Al_2O_3). However, all material classes studied (carbonaceous, fumed oxides, nanoscale metals, fine oxides, and miscellaneous) have dustiness values which range over at least an order of magnitude.

A strong linear relationship was observed between the total and respirable dustiness, with the respirable dustiness accounting for approximately one-third that of the total dustiness. It is believed that this relationship holds for many fine/nanoscale test powders (i.e. those selected for testing in this study) with this device but may not hold for coarse powders.

No relationship was observed between total or respirable dustiness and BET specific surface area, suggesting that primary particle size is not a factor in determining the dustiness of a powder. Particle size distributions (by number and aerodynamic diameter) for a subset of the test powders (measured simultaneously with an ELPI and an APS), indicated that particle size modes ranged from approximately 300 nm to several micrometers. No modes below 100 nm (aerodynamic diameter) were observed for the subset of materials measured, suggesting that it is unlikely that a substantial sub-100 nm fraction would be observed in a workplace.

Acknowledgements—We thank M. Boundy and D. Leith (UNC, Chapel Hill) for the fabrication and commissioning of the tester and for valuable discussions and assistance. We thank D. Bard, D. Mark, A.D. Maynard, and M.D. Hoover for helpful discussions; M. Miller for dustiness measurements of the lactose control; B. Jones for assistance with video graphic documentation. We thank Professor G. Oberdörster for the donations of the Printex 90 and Sterling V carbon blacks; Southwest Nanotechnologies for the donation of the SWeNT SWCNT; T. Polton (Pfizer) for the donation of the Holland lactose; T. Maher (AltairNano) for the donations of the lithium titanate spinel and of the titania (Kemira). We also acknowledge the assistance of K. Ashley, M. E. Birch, K. H. Dunn, C. Geraci, B.K. Ku, and the reviewers at *Annals*, for their comments in reviewing this article. This research was supported through the NIOSH Division of Applied Research and Technology and the NIOSH Nanotechnology Research Center.

Disclaimers—The findings and conclusions in this report are those of the authors and do not necessarily represent the views of the National Institute for Occupational Safety and Health. Mention of product or company name does not constitute endorsement by the Centers for Disease Control and Prevention. None of the authors has a financial relationship with a commercial entity that has an interest in the subject of this manuscript. The costs of publication of this article were defrayed in part by the payment of page charges. This article must therefore be marked 'advertisement', in accordance with 18 U.S.C. Section 1734, solely to indicate this fact.

REFERENCES

Andreasen AHM, Hoffman-Bang H, Rasmussen NH. (1939) On the ability of materials to be dusty. Kolloid-Zeitschrift; 86: 70–7 [in German].

ASTM. (1980). Test method for index of dustiness of coal and coke. American Society for Testing and Materials ASTM. D547–41 (withdrawn 1986).

Bach S, Schmidt E. (2008) Determining the dustiness of powders–a comparison of three measuring devices. Ann Occup Hyg; 52: 717–25.

Birch ME, Ku BK, Evans DE *et al.* (2011) Exposure and emissions monitoring during carbon nanofiber production–Part I: elemental carbon and iron-soot aerosols. Ann Occup Hyg; 55: 1016–26.

BOHS. (1985). Dustiness estimation methods for dry materials. Technical Guide No. 4. British Occupational Hygiene Society Technology Committee Working Group on Dustiness Estimation (Hammond CM, Heriot NR, Higman RW, Spivey AM, Vincent JH, Wells AB). Science Reviews Ltd.

BOHS. (1988). Progress in dustiness estimation. Ann Occ Hyg; 32: 535–44.

Boundy M, Leith D, Polton T. (2006) Method to evaluate the dustiness of pharmaceutical powders. Ann Occup Hyg; 50: 453–8.

Breum NO, Nielsen BH, Nielsen EM *et al.* (1997) Dustiness of compostable waste: a methodological approach to quantify the potential of waste to generate airborne micro-organisms and endotoxin. Waste Manag Res; 15: 169–87.

Breum NO. (1999) The rotating drum dustiness tester: variability in dustiness in relation to sample mass, testing time, and surface adhesion. Ann Occ Hyg; 43: 557–66.

Breum NO, Schneider T, Jørgensen O *et al.* (2003) Cellulosic building insulation versus mineral wool, fiberglass or perlite: installer's exposure by inhalation of fibers, dust, endotoxin and fire-retardant additives. Ann Occup Hyg; 47: 653–69.

Brouwer D. (2010) Exposure to manufactured nanoparticles in different workplaces. Toxicology; 269: 120–7.

Brouwer DH, Links IH, De Vreede SA *et al.* (2006) Size selective dustiness and exposure; simulated workplace comparisons. Ann Occup Hyg; 50: 445–52.

Brunauer S, Emmett PH, Teller E. (1938) J Am Chem Soc; 60: 309.

Carlson KH, Herman DR, Markey TF *et al.* (1992) A comparison of two dustiness evaluation methods. Am Ind Hyg Assoc J; 53: 448–54.

Cashdollar KL. (2000) Overview of dust explosibility characteristics. J Loss Prev Process Ind; 13: 183–99.

Cawley B, Leith D. (1993) Bench-top apparatus to examine factors that affect dust generation. Appl Occup Environ Hyg; 8: 624–31.

CEN. (2006) EN 15051 Workplace atmospheres: measurement of the dustiness of bulk materials; requirements and test methods. Brussels, Belgium: European Committee for Standardization.

Cheng L. (1973) Formation of airborne-respirable dust at belt conveyor transfer points. Am Ind Hyg Assoc J; 34: 540–6.

Chung KY, Burdett GJ. (1994) Dustiness testing and moving towards a biologically relevant dustiness index. Ann Occup Hyg; 38: 945–9.

Class P, Deghilage P, Brown RC. (2001) Dustiness of different high-temperature insulation wools and refractory ceramic fibres. Ann Occup Hyg; 45: 381–4.

Cowherd C Jr, Grelinger MA, Wong KF. (1989) Dust inhalation exposures from the handling of small volumes of powders. Am Ind Hyg Assoc J; 50: 131–8.

Dahm MM, Evans DE, Schubauer-Berigan MK *et al.* (2012) Occupational exposure assessment in carbon nanotube and nanofiber primary and secondary manufacturers. Ann Occup Hyg; 56: 542–56.

DIN. (1999). Determination of a parameter for the dust formation of pigments and extenders—Part 2: Drop Method. DIN 55992-2 [Deutsches Institut für Normung E.V. (German National Standard)]. Berlin: Beauth Verlag.

DIN. (2006). Determination of a parameter for the dust formation of pigments and extenders—Part 1: Rotation Method. DIN 55992-1 [Deutsches Institut für Normung E.V. (German National Standard)]. Berlin: Beauth Verlag.

Evans DE, Ku BK, Birch ME *et al.* (2010) Aerosol monitoring during carbon nanofiber production: mobile direct-reading sampling. Ann Occup Hyg; 54: 514–31.

Hamelmann F, Schmidt E. (2003) Methods for characterizing the dustiness estimation of powders—a review. KONA; 21: 7–18.

Hamelmann F, Schmidt E. (2004) Methods for characterizing the dustiness estimation of powders. Chem Eng Technol; 27: 844–7.

Hamelmann F, Schmidt E. (2005) Methods for dustiness estimation of industrial powders. China Particuology; 3: 90–3.

Hammond CM. (1980) Dust control concepts in chemical handling and weighing. Ann Occup Hyg; 23: 95–109.

Heitbrink WA, Todd WF, Fischbach TJ. (1989) Correlation of tests for material dustiness with worker exposure from the bagging of powders. Appl Ind Hyg; 4: 12–6.

Heitbrink WA, Todd WF, Cooper TC *et al.* (1990) The application of dustiness tests to the prediction of worker dust exposure. Am Ind Hyg Assoc J; 51: 217–23.

Heitbrink WA, Baron PA, Willeke K. (1992) An investigation of dust generation by free falling powders. Am Ind Hyg Assoc J; 53: 617–24.

Hinds WC. (1999) Aerosol Technology: properties, behavior and measurement of airborne particles. 2nd edn. New York: John Wiley and Sons Inc.

Hjemsted K, Schneider T. (1996a) Dustiness from powder materials. J Aerosol Sci; 27: S485–6.

Hjemsted K, Schneider T. (1996b) Documentation of a dustiness drum test. Ann Occ Hyg; 40: 627–43.

Ibaseta N, Climent E, Biscans B. (2008) Ultrafine aerosol generation from free falling nanopowders: experiments and numerical modeling. Int J Chem ReactorEng; 6: Article A24.

ISO 14488. (2007) Particulate materials: sampling and sample splitting for the determination of particulate properties.

Jensen KA, Koponen IK, Clausen PA, Schneider T. (2009) J Nanopart Res; 11: 133–46.

Kenny LC, Gussman RA. (1997) Characterization and modeling of a family of aerosol preseparators. J Aerosol Sci; 28: 677–88.

Ku BK, Emery MS, Maynard AD *et al.* (2006) In situ structure characterization of airborne carbon nanofibres by a tandem mobility-mass analysis. Nanotechnology; 17: 3613–21.

Lanning JS, Boundy MG, Leith D. (1995) Validating a model for the prediction of dust generation. Particulate Sci Technol; 13: 105–16.

Lidén G. (2006) Dustiness testing of materials handled at workplaces. Ann Occup Hyg; 50: 437–9.

Mark D. (2005) The use of reliable measurements of dustiness of chemicals in selecting the most appropriate dust control technology. Presented at the 6th International Scientific Conference of the International Occupational Hygiene Association, North West Province, South Africa. 19–23 September 2005. Paper S2–S3.

NIOSH (2010) *Occupational Exposure to Carbon Nanotubes and Nanofibers*. Current Intelligence Bulletin draft. Available at http://www.cdc.gov/niosh/docket/review/docket161a/. Accessed Aug 20th 2012.

NIOSH (2011) *Occupational Exposure to Titanium Dioxide*. Current Intelligence Bulletin 63. http://www.cdc.gov/niosh/docs/2011-160/pdfs/2011-160.pdf. Accessed Aug 20th 2012.

O'Shaughnessy PT, Kang M, Ellickson D. (2012) A novel device for measuring respirable dustiness using low-mass powder samples. J Occup Environ Hyg; 9: 129–39.

Paik SY, Zalk DM, Swuste P. (2008) Application of a pilot control banding tool for risk level assessment and control of nanoparticle exposures. Ann Occup Hyg; 52: 419–28.

Pensis I, Mareels J, Dahmann D *et al.* (2010) Comparative evaluation of the dustiness of industrial minerals according to European standard EN 15051, 2006. Ann Occup Hyg; 54: 204–16.

Petavratzi E, Kingman SW, Lowndes IS. (2006) Assessment of the dustiness and the dust liberation mechanisms of limestone quarry operations. Chem Eng Processing; 46: 1412–23.

Peters TM, Elzey S, Johnson R *et al.* (2009) Airborne monitoring to distinguish engineered nanomaterials from incidental particles for environmental health and safety. J Occup Environ Hyg; 6: 73–81.

Plinke MA, Leith D, Holstein DB *et al.* (1991) Experimental examination of factors that affect dust generation. Am Ind Hyg Assoc J; 52: 521–8.

Plinke MA, Maus R, Leith D. (1992) Experimental examination of factors that affect dust generation by using Heubach and MRI testers. Am Ind Hyg Assoc J; 53: 325–30.

Plinke MAE, Leith D, Goodman RG *et al.*. (1994a) Particle separation mechanisms in flow of granular material. Particulate Sci Technol; 12: 71–87.

Plinke MAE, Leith D, Löffler F. (1994b) Cohesion in granular materials. Bulk Solids Handling; 14: 101–6.

Plinke MAE, Leith D, Boundy MG *et al.* (1995) Dust generation from handling powders in industry. Am Ind Hyg Assoc J; 56: 251–7.

Ruda-Eberenz T.A., Birch M.E., Chai M. Specific Surface Areas of Commercially Produced Carbon Nanomaterials. Ann. Occup. Hyg, in press.

Schneider T, Jensen KA. (2008) Combined single-drop and rotating drum dustiness test of fine to nanosize powders using a small drum. Ann Occup Hyg; 52: 23–34.

Schulte P, Geraci C, Zumwalde R *et al.* (2008) Occupational risk management of engineered nanoparticles. J Occup Environ Hyg; 5: 239–49.

Shvevdova AA, Kisin ER, Mercer R *et al.* (2005) Unusual inflammatory and fibrogenic pulmonary responses to single-walled carbon nanotubes in mice. Am J Physiol Lung Cell Mol Physiol; 289: L698–708.

Shvevdova AA, Kisin E, Murray AR *et al.* (2008) Inhalation vs. aspiration of single-walled carbon nanotubes in C57BL/6 mice: inflammation, fibrosis, oxidative stress, and mutagenesis. Am J Physiol Lung Cell Mol Physiol; 295: L552–65.

Sutter SL, Johnson JW, Mishima J. (1982) Investigation of accident-generated aerosols: releases from free fall spills. Am Ind Hyg Assoc J; 43: 540–3.

Tsai C-J, Huang C-Y, Chen S-C *et al.* (2011) Exposure assessment of nano-sized and respirable particles at different workplaces. J Nanopart Res; 13: 4161–72.

Tsai CJ, Wu CH, Leu ML, Chen SC, Huang CY, Tsai PJ, Ko FH (2009) Dustiness test of nanopowders using a standard rotating drum with a modified sampling train. J Nanopart Res 11(1): 121–131.

Turkevich LA, Fernback JE, Dastidar AG. Potential explosive hazard of carbonaceous nanoparticles, in preparation.